

AMCoR

Asahikawa Medical University Repository <http://amcor.asahikawa-med.ac.jp/>

The American journal of pathology (2009.Mar) 174卷3号:881~890.

Suppressive effect of orthovanadate on hepatic stellate cell activation and liver fibrosis in rats

Yuji Nishikawa, Naoto Ohi, Akiko Yagisawa, Yuko Doi,
Yohei Yamamoto, Masayuki Yoshida, Takuo Tokairin,
Toshiaki Yoshioka, Yasufumi Omori, Katsuhiko Enomoto

Suppressive effect of orthovanadate on hepatic stellate cell activation and liver fibrosis in rats

Yuji Nishikawa, Naoto Ohi, Akiko Yagisawa, Yuko Doi,* Yohei Yamamoto, Masayuki Yoshida, Takuo Tokairin, Toshiaki Yoshioka, Yasufumi Omori, and Katsuhiko Enomoto

From the Department of Pathology and Central Research Laboratory,* Akita University School of Medicine, 1-1-1 Hondo, Akita 010-8543, Japan

Running head: Stellate cell suppression by orthovanadate

This work was supported in part by grants from the Ministry of Education, Science, Sports and Culture of Japan (#16590303 and #18590362).

Address reprint requests to Yuji Nishikawa, Department of Pathology, Akita University School of Medicine, 1-1-1 Hondo, Akita 010-8543, Japan. Phone: +81-18-884-6061; Fax: +81-18-836-2601; E-mail: nishikwa@med.akita-u.ac.jp

Abstract

Orthovanadate (OV), an inhibitor of protein tyrosine phosphatases, affects various biological processes in a cell type-specific manner. Here we investigated the effect of OV on hepatic stellate cells (HSCs). When primary rat HSCs were cultured in the presence of 10% serum, they spontaneously proliferated and transformed into the activated state with formation of abundant stress fibers and increased expression of α -smooth muscle actin (α -SMA) and collagen type I mRNA. OV treatment inhibited proliferation and activation of HSCs and partially reversed the phenotype of activated HSCs. Among the signaling molecules investigated, phosphorylation of the Src protein at tyrosine 416 was the most striking in OV-treated HSCs. Treatment of cells with Src family inhibitors partly abrogated the effect of OV. The activity of Rho, which is known to be negatively regulated by Src, was increased in the activated HSCs but remained at lower levels in OV-treated cells. We then examined whether OV was effective in suppression of HSC activation *in vivo* after liver injury induced by carbon tetrachloride or dimethylnitrosamine. OV significantly reduced the appearance of α -SMA-positive cells and decreased collagen deposition, with improvement of liver function. Our study showed for the first time that OV suppressed the activation of HSCs, possibly through modulation of Src and Rho activities, and attenuated fibrosis after chronic liver injuries.

Introduction

Vanadium is an ultratrace element in vertebrates and its total body store is estimated to be about 100 µg in humans.¹ In the biological system, vanadium is found predominantly as vanadate (+5; orthovanadate [OV] and metavanadate) or vanadyl (+4), with the transition between these forms in the cytoplasm.² Although its essentiality has not been proved in humans, it is considered to have many regulatory roles in the body. Exogenously administered vanadium compounds have been shown to exert various biological effects, most notably, insulin-mimetic actions.³

The biological actions of the vanadium compounds are complex and their exact mechanisms remain elusive. However, in the case of OV, which has a phosphate-like structure, the inhibition of various phosphoryl transfer enzymes, including protein tyrosine phosphatases (PTPs) and ATPases, could be the most relevant to the biological effects.^{1,3} In particular, OV has been shown to bind to the active center of protein tyrosine phosphatases,⁴ thereby strongly inhibiting their activity and inducing a prolonged state of increased protein tyrosine phosphorylation of cellular proteins.^{5,6} At least part of the insulin-mimetic action is attributable to inhibition of protein tyrosine phosphatases.⁷

We previously demonstrated that OV enhanced branching morphogenesis and proliferation of rat hepatocytes cultured within collagen gels,⁸ and that it prevented apoptotic death of rat endothelial sinusoidal cells.⁹ In long-term cultures of rat hepatocytes,⁸ we noticed that OV almost completely prevented proliferation of

contaminated hepatic stellate cells (HSCs) in the hepatocyte fraction. This prompted us to investigate the effect of OV on purified rat HSCs. In the present study, we have shown that OV strongly inhibits proliferation of rat HSCs and liver fibrosis, and proposed the possible mechanisms of the action.

Materials and Methods

Isolation and culture of ratHSCs. HSCs of aged male F344 rats were isolated by pronase-collagenase perfusion and subsequent purification by a single-step Nycodenz gradient.¹⁰ Isolated HSCs were plated onto collagen-coated plastic dishes and cultured in Williams' E medium supplemented with 10% fetal bovine serum and 10 mM nicotinamide. All the animal experiments adhered to the criteria outlined in the *Guide for the Care and Use of Laboratory Animals* prepared by the Institute of Laboratory Animal Resources Commission on Life Sciences, National Research Council (National Academy Press, 1996).

To examine the effects of increased protein tyrosine phosphorylation on HSC activation, OV (sodium orthovanadate, Wako Pure Chemical, Osaka, Japan; dissolved in saline) was added to the medium at various concentrations 3 hours after plating. OV was also applied to HSCs activated by culturing for 7 to 10 days. The number of cells per well was estimated by Hoechst 33258-based DNA fluorometric assay after 7 days. In some experiments, Src family inhibitors (PP1 and PP2, Calbiochem, San Diego, CA) and an inhibitor of ROCK (p160-Rho-associated coiled-coil-containing protein kinase)

(Y-27632, Sigma-Aldrich, St. Louis, MO) were applied.

Western blot analysis. Protein samples extracted from HSCs were electrophoresed in 10% polyacrylamide gels (40 µg per lane) and transferred to PVDF membranes.

Primary antibodies used were anti- α -smooth muscle actin (α -SMA) (DAKO, Carpinteria, CA), anti-desmin (Sanbio, Uden, The Netherlands), anti-vimentin (DAKO), anti-proliferating cell nuclear antigen (PCNA) (Santa Cruz Biotechnology, Santa Cruz, CA), glyceraldehyde 3-phosphate dehydrogenase (GAPDH) (Chemicon International, Temecula, CA), anti-phosphotyrosine (P-Tyr-100; Cell Signaling Technology, Beverly, MA), anti-phospho-ERK (Santa Cruz Biotechnology), anti-phospho-p90RSK (Cell Signaling Technology), anti-phospho-Akt (Cell Signaling Technology), anti-phospho-Stat3, anti-phospho-p38 MAPK (Cell Signaling Technology), anti-phospho-CREB (Cell Signaling Technology), anti-Src (Src, phospho-Src [Tyr416], phospho-Src [Tyr527]; Cell Signaling Technology), anti-Rho (Cytoskeleton, Denver, CO), anti-Rac (Cytoskeleton), and anti-Cdc42 (Santa Cruz Biotechnology). Detection was performed with enhanced chemiluminescence reagents (GE Healthcare, Buckinghamshire, UK).

Reverse transcriptase-polymerase chain reaction (RT-PCR). Total RNA from cultured HSCs was prepared by using a TRIzol reagent (Invitrogen-Life Technologies, Carlsbad, CA) and RT-PCR analysis was performed. A one-step RT-PCR kit (TaKaRa, Ohtsu,

Japan) was used for the reaction, in which RNA (0.2 µg/20 µl reaction) was reverse transcribed using AMV reverse transcriptase for 30 min and then amplified for 25 cycles of 95, 60, and 72°C for 30, 30, and 90 seconds, respectively. The specific primers used and the expected fragment sizes were as follows. Collagen type Iα (Coll-Iα): forward, 5'-CAAGATGGCATCCCTGGACAG-3'; reverse, 5'-AGCTGCACCGACAGCACCATC-3'; 600 bp. Fibronectin: forward, 5'-TGCAATGATCAGGACACCAGG-3'; reverse, 5'-GTAATTCCGGTTGCTGTACAG-3', 600 bp. Plasminogen activator inhibitor I (PAI-I): forward, 5'-CAGCTCCTGCCCTCCGAAAGC-3'; reverse, 5'-GTTGAACTTGTTGTTCTGAGCC-3'; 416 bp. Peroxisome proliferator-activated receptor γ (PPARγ): forward, 5'-AGCATCAGGCTTCCACTATGG-3'; reverse, 5'-GATCGAAACTGGCACCCTTGA-3'; 517 bp. c-Myb: forward, 5'-TGGCAGAAAGT(A/G)CT(A/G)AACCCCT-3'; reverse, 5'-TCCAGTGGTTCTTGATAGCA-3'; 313 bp.¹¹ GAPDH: forward, 5'-ACCACAGTCCATGCCATCAC-3'; reverse, 5'-TCCACCACCCTGTTGCTGTA-3'; 452 bp.

Immunocytochemistry, F-actin staining, and sirius red staining.

Immunocytochemistry for α-SMA and desmin was performed on methanol-fixed cultured cells or paraffin sections of formalin-fixed liver tissues. Detection was performed with an LSAB kit (DAKO). F-actin was visualized by rhodamine-phalloidin

(Invitrogen-Molecular Probes, Carlsbad, CA). Sirius red staining was used to estimate the extent of liver fibrosis.

Activation assay for the Rho family proteins. Lysates of HSCs were incubated with rhotekin-conjugated beads (for Rho; Cytoskeleton) or p21-associated kinase-conjugated beads (for Rac and Cdc42; Cytoskeleton) for 2 hours at 4°C. After washing the beads, the GTP-bound forms were eluted by boiling in SDS sample buffer and visualized by Western blot analysis.

Induction of liver injury and fibrosis. In an acute liver injury model, a 1:1 mixture of CCl₄ and olive oil (or olive oil for control) was administered by gavage at a dose of 3 ml/kg body weight. The animals were sacrificed 24, 48, and 72 hrs after CCl₄ treatment. OV (5 mg/kg) or saline was injected intraperitoneally at 30 minutes before CCl₄ treatment. Additional OV or saline injections were performed 24 hrs (for animals sacrificed after 48 hrs) and 24 and 48 hrs (for animals sacrificed after 72 hrs) after CCl₄ treatment.

To induce chronic liver injury, CCl₄ was administered by gavage at a dose of 1 ml/kg twice per week for 8 weeks. OV was injected intraperitoneally at the doses of 2, 4, and 8 mg/kg, three times per week. Another chronic liver injury model induced by dimethylnitrosamine (DMN) was also used. DMN (1% in saline) was intraperitoneally injected at a dose of 1 ml/kg, three times per week, for 5 weeks. OV (2.5, 5, and 10

mg/kg) was intraperitoneally injected three times per week.

The levels of serum transaminases (alanine aminotransferase [ALT] and aspartate aminotransferase [AST]) and alkaline phosphatase (ALP) were measured by the DriChem System (Fujifilm, Tokyo, Japan). The extent of fibrosis (sirius red stained area) and HSC activation (α -SMA- and desmin-immunoreactivity) was quantified using morphometry software (KSW-500U, Kurabo, Osaka, Japan).

Hydroxyproline assay. In the chronic liver injury models, hepatic collagen content was evaluated by hydroxyproline quantification according to the method described by Edwards and O'Brien¹² with some modifications. The liver tissues (75 to 100 mg) were homogenized in 1 ml of phosphate-buffered saline and hydrolyzed in 6 N HCl overnight at 120°C. Five μ l of hydrolysates were mixed with the same amount of citrate acetate buffer, and then 100 μ l of chloramin T solution was added. After 20 minutes of incubation at room temperature, 100 μ l of Ehrlich's solution was added. The mixtures were incubated for 15 minutes at 65°C and then absorbance was read at 550 nm. A standard curve was prepared with purified hydroxyproline (Sigma). The hepatic hydroxyproline content was expressed as μ g/g wet liver weight.

Results

OV inhibits HSC proliferation and activation in vitro. After being plated, HSCs spontaneously demonstrated an activated phenotype and began to proliferate (Fig. 1A).

OV inhibited their proliferation dose-dependently (Fig. 1A, B) and maintained the stellate morphology characteristic of quiescent HSCs (Fig. 2). Abundant stress fibers were present in the extended cytoplasm of the activated HSCs, but their amount was much less in the OV-treated cells (Fig. 2). OV partially retained the retinol uptake capacity that was lost in activated HSCs (Fig. 2).

Expression of α -SMA protein, the most reliable marker for HSC activation, became apparent after 7 days in control HSCs, but the expression was almost completely inhibited in cells treated with OV (Fig. 3A). Immunocytochemical analysis of 14 day-cultured HSCs also demonstrated the suppressive effect of OV on α -SMA expression (Fig. 2). While expression of desmin protein, a marker for both quiescent and activated HSCs,¹³ gradually increased in cultured cells, it was only modestly inhibited by OV (Fig. 3A). Expression levels of vimentin protein were not affected by OV (Fig. 3A). As expected from the inhibitory effect on HSC proliferation, OV inhibited expression of PCNA protein (Fig. 3A).

In the activated HSCs, gene expression of collagen type I α , fibronectin, and PAI-I was increased, while that of PPAR γ was decreased (Fig. 3B). Gene expression of collagen type I α was strongly inhibited by OV, although expression of other genes was not affected (Fig. 3B). OV also inhibited c-Myb gene expression, which is known to positively regulate differentiation toward smooth muscle cells (Fig. 3B).¹⁴

To examine whether OV could reverse the activated phenotype of HSCs, cells were activated by culturing 7 to 10 days and then cultured for additional 7 days in the

presence of OV. After addition of OV, extended cytoplasm rich in stress fibers gradually shrank and arborizing fine cellular processes emerged, and they recovered the stellate morphology similar to quiescent cells (Fig. 4A). These morphological changes were accompanied by a decrease in the expression of α -SMA, PCNA, and collagen type I α (Fig. 4B).

OV induces Src phosphorylation at tyrosine 416 in cultured HSCs. There was a general increase in protein tyrosine phosphorylation levels in OV-treated HSCs (Fig. 5A). Phospho-specific Western blot analysis revealed that the phosphorylation levels of ERK, p190RSK, Akt, and Stat3 were increased, while those of p38 MAPK and CREB were decreased in the activated HSCs (Fig. 5B). OV treatment enhanced phosphorylation of p190RSK, Akt, and Stat3, but the extents were at most mild to moderate, and the phosphorylation levels of ERK, p38 MAPK, and CREB were not affected (Fig. 5B).

We next examined the phosphorylation status of Src, whose activity has been shown to be regulated by phosphorylation of several tyrosine residues.¹⁵ While Src was autophosphorylated at tyrosine 416 in the freshly isolated HSCs, it was markedly dephosphorylated during culture (Fig. 6A). In the presence of OV, however, tyrosine 416 phosphorylation was maintained (Fig. 6A). Src phosphorylation at tyrosine 527 increased during culture, but the extent was small and only mildly enhanced by OV (Fig. 6A). Both PP1 and PP2 strongly inhibited the OV-induced morphological changes

(PP2, Fig. 6B; PP1, data not shown). Furthermore, PP2 partially abrogated the inhibition of α -SMA expression by OV (Fig. 6C).

OV inhibits activation of the Rho protein family in cultured HSCs. Since Src is known to regulate the function of Rho protein, which plays important roles in actin remodeling and myogenic differentiation of HSCs,^{16,17} we investigated the activation status of the Rho protein family in cultured HSCs. Rho, Rac, and Cdc42 were present in quiescent HSCs, but they scarcely bound to rhotekin- or p21-associated kinase-conjugated beads, indicating that they were largely in the inactive, GDP-bound state (Fig. 7A). In cultured and activated cells, there was an increase in the active (GTP-bound) forms of these proteins (Fig. 7A). In the OV-treated cells, however, the amount of active forms was reduced to a level comparable to that of quiescent cells (Fig. 7A). Inhibition of the Rho signaling pathway by a ROCK inhibitor, Y-27632, induced a stellate morphology that was similar to that in OV-treated HSCs (Fig. 7B).

OV inhibits myofibroblastic transformation of HSCs in vivo and suppresses liver fibrosis. CCl₄ treatment caused a marked increase in transaminases and centrilobular necrosis to a similar extent in saline- and OV-treated animals (ALT levels: Supplemental Fig. 1; histology: Fig. 8A). The appearance of α -SMA-positive HSCs, which occurred after 72 hours in the control, was dramatically suppressed, while α -SMA expression in vascular smooth muscle cells was maintained (Fig. 8A, B).

Although OV did not affect the appearance of desmin-positive HSCs in the necrotic area at 2 days, a further increase in desmin-positive cells was inhibited by OV (Fig. 8A, B).

We then examined the effect of OV in a chronic CCl₄ injury model. Chronic OV treatment (5 mg/kg, three times per week; 8 weeks) did not induce any physical symptoms or behavioral alterations and there were no discernible histological abnormalities in major organs, including the liver, pancreas, kidneys, spleen, heart, and lungs (Supplemental Fig. 2). After repeated CCl₄ treatments for 8 weeks, a marked body weight loss occurred, but it was ameliorated by OV treatment (olive oil: 278.3±3.5 g; 4 mg/kg OV: 270.3±2.6 g; CCl₄: 211.9±8.9 g, CCl₄+OV: 244.2±6.1 g). In animals treated with CCl₄ only, the liver became shrunken and increased its consistency (Fig. 9A), and the serum levels of transaminases (ALT and AST) and alkaline phosphatase (ALP) were elevated (Fig. 9B; AST, data not shown). The elevated levels of these enzymes were due to accumulated effects of repeated CCl₄ administrations, since animals were sacrificed after 4 days after the last CCl₄ administration, when transaminase levels should return to near normal after a single administration of CCl₄, which was confirmed in a separate experiment (data not shown). However, administration of OV improved the gross appearances of the liver (Fig. 9A) and inhibited the elevation of the transaminases and ALP dose-dependently (Fig. 9B). Histological analysis revealed that cirrhotic changes with lobular remodeling in the liver of CCl₄-treated rats were markedly ameliorated by OV treatment (Fig. 9C). This antifibrogenic effect of OV was

dose-dependent and statistically significant (Fig. 9D). Quantification of hepatic hydroxyproline content confirmed the effect of OV treatment (Fig. 9D).

The effect of OV was further examined in a chronic DMN model. The livers in DMN-treated animals were shrunken with dark discoloration due to congestion, while OV treatment decreased these gross abnormalities (Fig. 10A). DMN treatment elevated the levels of transaminases and ALP, but they were significantly decreased by OV treatment (Fig. 10B). As in the chronic CCl₄ injury model, the elevated levels of these enzymes were due to accumulated effects of DMN administrations, since animals were sacrificed after 5 days after the last DMN administration, when transaminase levels usually returned to near normal after a single administration of DMN. While chronic DMN treatment increased delicate collagen fibers and α -SMA-positive HSCs along the hepatic sinusoids (Fig. 10C), OV treatment significantly reduced the extent of collagen deposition, as well as the appearance of α -SMA-positive cells (Fig. 10C, D).

Discussion

In the present study, we showed that OV exerted strong suppressive effect on HSC activation *in vitro* and *in vivo*. One of the interesting features of the biological effect of OV is its prolonged stimulation of tyrosine phosphorylation of many proteins.^{5,6,18} We reported that OV enhanced bile duct-like branching morphogenesis of hepatocytes within collagen gels, which was mainly attributable to stimulation of the MEK-ERK and PI3K-Akt pathways.⁸ We also found that OV suppressed apoptosis of

liver sinusoidal endothelial cells through the maintenance of Bad phosphorylation by stimulation of MEK-ERK, p38 MAPK, and PI3K-Akt pathways.⁹ In contrast to the cases of hepatocytes and sinusoidal endothelial cells, OV did not or only modestly affect the phosphorylation status of ERK, Akt, and p38 MAPK in HSCs, indicating that the effect of OV is cell type-specific or context-dependent.

Despite the significant inhibitory effects on the expression of α -SMA and stress fiber formation, as well as on collagen production and proliferation, OV did not suppress the molecular changes that have been known to closely associate with HSC activation, such as dephosphorylation of CREB,¹⁹ decreased PPAR- γ expression,²⁰ and increased PAI-I expression.²¹ While these established mechanisms for HSC activation may act independently or cooperatively to induce activated phenotype of HSCs, our results suggest that OV might act more directly to the mechanism of actin remodeling with α -SMA expression, which is among the most essential characteristics of activated HSCs. The strong effect of OV on α -SMA inhibition might also relate to its effect on gene expression of c-Myb that has been demonstrated to positively regulate differentiation to smooth muscle cells.¹⁴

There was considerable Src phosphorylation at tyrosine 416 in freshly isolated HSCs, but its level was decreased during activation in culture. In contrast, the phosphorylation level of tyrosine 527 increased only modestly during culture. It has been demonstrated that autophosphorylation of tyrosine 416 stimulates Src activity, while phosphorylation of tyrosine 527 inhibits it,¹⁵ rendering its activity dependent on

the balance of phosphorylation of these two sites.²² Thus, our results suggest that Src activity is high in quiescent HSCs, but decreased when cells are activated. Although there has been a report suggesting that the src kinase pathway might contribute to HSC activation via inducing thrombospondin-1 and transforming growth factor- β 1,²³ several studies have implicated the possible link between HSC activation and a decrease in Src activity. It has been described that Src kinase activity in cultured human HSCs is high in the quiescent state (nonadherent condition), while the activity is reduced when activated (adherent condition).²⁴ The suppression of Src activity during activation might be mediated by a cell surface glycoprotein (Thy-1),²⁵ which increases in myofibroblasts after liver injuries.²⁶ Furthermore, there might be a possibility that an increased activity of cell surface transglutaminase, which is associated with HSC activation, induces integrin clustering and suppresses Src activity.²²

OV induced marked autophosphorylation of Src at tyrosine 416, while it only mildly increased tyrosine 527 phosphorylation, suggesting that OV might maintain or stimulates the activity in HSCs. Our data showing that the effect of OV on HSCs was partly abrogated by the Src family inhibitors support the importance of Src activation in the action of OV. Although incubation of fibroblastic cells with OV has been shown to inhibit Src activity by increasing tyrosine 527 phosphorylation,²⁷ the apparently contradictory results may be due to short-term incubation in the study, since the effect of OV on protein tyrosine phosphorylation in viable cells in culture proceeds slowly

and steadily for more than 6 hours¹⁸ and continues for at least several days.^{8,9}

Alternatively, since it has been shown that distinct PTPs regulate the phosphorylation status of these two tyrosine residues,¹⁵ the preferential effect on tyrosine phosphorylation may be due to a specific PTP expression profile in HSCs.

Activation of HSCs was associated with an increase in the GTP-bound forms of Rho, Rac, and Cdc42, while these were significantly decreased in OV-treated cells. The antiproliferative activity of OV is consistent with the roles of the Rho family proteins in mediating adhesion-dependent cell cycle progression.²⁸ It has also been suggested that Rho activation is involved in the myofibroblastic differentiation of activated HSCs.^{16,17} The activity of Rho is known to be regulated by Src, which phosphorylates and activates one of the substrates, p190 RhoGAP, enhancing the conversion of Rho-GTP to Rho-GDP and blocking stress fiber formation.^{22,29,30} Since the activity of p190 RhoGAP is negatively regulated by a PTP containing Src homology 2 (SHP2),³¹ it might also be possible that OV enhances the activity of p190 RhoGAP through SHP2 inhibition. A specific ROCK inhibitor (Y-27632), which has been shown to inhibit activation of HSCs both *in vitro*³² and *in vivo*,³³ induced dendritic morphological changes similar to those induced by OV. This may further suggest the importance of inhibition of the Rho signaling pathway in the maintenance and restoration of the quiescent state of HSCs. Furthermore, inhibition of Rac activation by OV might also be relevant to inhibition of HSC activation, since sustained activation of Rac1 has been suggested to promote HSC activation and liver fibrosis.³⁴

In agreement with the *in vitro* observations of OV's actions on HSCs, OV showed antifibrotic effects *in vivo* in liver injuries induced by two different hepatotoxic agents. Although our study suggests that HSCs are the major targets of OV in its antifibrotic effects, the protective effects *in vivo* could be more complex. It is also possible that OV protects other types of cells in the liver, such as sinusoidal endothelial cells, hepatocytes, and Kupffer cells. In fact, as we previously mentioned, systemic treatment with OV exerted strong anti-apoptotic effects on sinusoidal endothelial cells in an ischemia-reperfusion liver injury model.⁹ In the present study, although OV did not apparently reduce hepatocyte injury *per se* (see Supplemental Fig. 1), it lowered the levels of transaminases and alkaline phosphatase in the chronic liver injury models. OV could protect hepatocytes either indirectly through improvement of the hepatic microenvironment or directly through influencing their cellular conditions. It is possible that OV might affect regenerative capacity of hepatocytes, since OV has been shown to release contact inhibition of cultured hepatocytes by inhibiting a protein tyrosine phosphatase (LAR), which is associated with and inactivates c-Met.³⁵ Furthermore, OV has been shown to affect Kupffer cell functions by inducing tyrosine phosphorylation of GTPase-activating protein.³⁶

In our animal experiments, despite attenuation of myofibroblastic transformation of HSCs by OV treatment, tissue repair was not hampered but rather facilitated, resulting in better gross and microscopic appearances of the liver with fewer biochemical abnormalities. Interestingly, similar observations have been made in

tendon repair.^{37,38} In these studies, OV inhibited differentiation of fibroblasts to α -SMA-positive myofibroblasts, but normal wound contraction took place with more rapid and orderly organization of collagen fiber bundles. While activation of HSCs could be a prerequisite for tissue repair following liver injuries, excessive myofibroblastic activation of HSCs may be harmful, resulting in liver fibrosis and cirrhosis.³⁹

Although vanadium compounds are normally present in animals including human and the essentiality has been proved in lower species,⁴⁰ there have been several reports showing that vanadium compounds may exert harmful effects, such as nephrotoxicity, when administered in excess.⁴¹ It has also been shown that orthovanadate transiently stimulates proliferation of cultured human mesangial cells.⁴² In our study, despite a slight decrease in body weight at higher doses, examination of major organs in chronically OV-treated animals revealed no evidence of pathological changes, including mesangial proliferation in the kidney. Furthermore, since it has been shown that the biological effect of OV is augmented by interaction with hydrogen peroxide by forming peroxivanadate,⁴³ hydrogen peroxide locally produced in the injured and inflamed sites⁴⁴ might enable OV to act at relatively low dosages without causing systemic adverse effects. It has been demonstrated that various organically chelated vanadium compounds are more potent in its insulin-mimetic action and less toxic.³ Further studies are required to examine whether such compounds might be beneficial in suppression of HSC activation and liver fibrosis.

In conclusion, the present study has demonstrated for the first time that OV suppressed HSC activation and liver fibrosis, and suggests that the underlying mechanisms may include modulation of the activity of Rho through Src activation. These findings, together with our previous observations on protective effects on ischemia-reperfusion liver injuries,⁹ suggest that OV or other vanadium compounds might offer therapeutic potential in liver diseases. Our results also highlight the potential importance of regulating the activities Src kinase in the suppression of HSC activation, which might be a clue to develop new therapeutic strategies.

Acknowledgements:

We appreciate the excellent technical assistance from Ms. E. Kumagai, Ms. R. Ito, and M. Kawamata.

References

1. Verma S, Cam MC, McNeill JH. Nutritional factors that can favorably influence the glucose/insulin system: vanadium. *J Am Coll Nutr* 1998; 17:11-18.
2. Li J, Elberg G, Crans DC, Shechter Y. Evidence for the distinct vanadyl(+4)-dependent activating system for manifesting insulin-like effects. *Biochemistry* 1996; 35:8314-8318.
3. Thompson KH, Orvig C. Vanadium in diabetes: 100 years from Phase 0 to Phase I. *J Inorg Biochem* 2006; 100:1925-1935.
4. Denu JM, Lohse DL, Vijayalakshmi J, Saper MA, Dixon JE. Visualization of intermediate and transition-state structures in protein-tyrosine phosphatase catalysis. *Proc Natl Acad Sci U S A* 1996; 93:2493-2498.
5. Swarup G, Cohen S, Garbers DL. Inhibition of membrane phosphotyrosyl-protein phosphatase activity by vanadate. *Biochem Biophys Res Commun* 1982; 107:1104-1109.
6. Klarlund JK. Transformation of cells by an inhibitor of phosphatases acting on phosphotyrosine in proteins. *Cell* 1985; 41:707-717.
7. Huyer G, Liu S, Kelly J, Moffat J, Payette P, Kennedy B, et al. Mechanism of inhibition of protein-tyrosine phosphatases by vanadate and pervanadate. *J Biol Chem* 1997; 272:843-851.
8. Nishikawa Y, Doi Y, Watanabe H, Tokairin T, Omori Y, Su M, et al. Transdifferentiation of mature rat hepatocytes into bile duct-like cells in vitro.

- Am J Pathol 2005; 166:1077-1088.
9. Ohi N, Nishikawa Y, Tokairin T, Yamamoto Y, Doi Y, Omori Y, et al. Maintenance of Bad phosphorylation prevents apoptosis of rat hepatic sinusoidal endothelial cells in vitro and in vivo. Am J Pathol 2006; 168:1097-1106.
 10. Schafer S, Zerbe O, Gressner AM. The synthesis of proteoglycans in fat-storing cells of rat liver. Hepatology 1987; 7:680-687.
 11. Jarvis TC, Alby LJ, Beaudry AA, Wincott FE, Beigelman L, McSwiggen JA, et al. Inhibition of vascular smooth muscle cell proliferation by ribozymes that cleave c-myb mRNA. Rna 1996; 2:419-428.
 12. Edwards CA, O'Brien WD, Jr. Modified assay for determination of hydroxyproline in a tissue hydrolyzate. Clin Chim Acta 1980; 104:161-167.
 13. Yokoi Y, Namihisa T, Matsuzaki K, Miyazaki A, Yamaguchi Y. Distribution of Ito cells in experimental hepatic fibrosis. Liver 1988; 8:48-52.
 14. Buck M, Kim DJ, Houglum K, Hassanein T, Chojkier M. c-Myb modulates transcription of the alpha-smooth muscle actin gene in activated hepatic stellate cells. Am J Physiol Gastrointest Liver Physiol 2000; 278:G321-328.
 15. Roskoski R, Jr. Src kinase regulation by phosphorylation and dephosphorylation. Biochem Biophys Res Commun 2005; 331:1-14.
 16. Yee HF, Jr. Rho directs activation-associated changes in rat hepatic stellate cell morphology via regulation of the actin cytoskeleton. Hepatology 1998;

- 28:843-850.
17. Kato M, Iwamoto H, Higashi N, Sugimoto R, Uchimura K, Tada S, et al. Role of Rho small GTP binding protein in the regulation of actin cytoskeleton in hepatic stellate cells. *J Hepatol* 1999; 31:91-99.
 18. Nishikawa Y, Wang Z, Kerns J, Wilcox CS, Carr BI. Inhibition of hepatoma cell growth in vitro by arylating and non-arylated K vitamin analogs. Significance of protein tyrosine phosphatase inhibition. *J Biol Chem* 1999; 274:34803-34810.
 19. Houghlum K, Lee KS, Chojkier M. Proliferation of hepatic stellate cells is inhibited by phosphorylation of CREB on serine 133. *J Clin Invest* 1997; 99:1322-1328.
 20. Miyahara T, Schrum L, Rippe R, Xiong S, Yee HF, Jr., Motomura K, et al. Peroxisome proliferator-activated receptors and hepatic stellate cell activation. *J Biol Chem* 2000; 275:35715-35722.
 21. Leyland H, Gentry J, Arthur MJ, Benyon RC. The plasminogen-activating system in hepatic stellate cells. *Hepatology* 1996; 24:1172-1178.
 22. Janiak A, Zemskov EA, Belkin AM. Cell surface transglutaminase promotes RhoA activation via integrin clustering and suppression of the Src-p190RhoGAP signaling pathway. *Mol Biol Cell* 2006; 17:1606-1619.
 23. Breitkopf K, Sawitza I, Gressner AM. Characterization of intracellular pathways leading to coinduction of thrombospondin-1 and TGF-beta1 expression in rat hepatic stellate cells. *Growth Factors* 2005; 23:77-85.

24. Carloni V, Defranco RM, Caligiuri A, Gentilini A, Sciammetta SC, Baldi E, et al. Cell adhesion regulates platelet-derived growth factor-induced MAP kinase and PI-3 kinase activation in stellate cells. *Hepatology* 2002; 36:582-591.
25. Barker TH, Grenett HE, MacEwen MW, Tilden SG, Fuller GM, Settleman J, et al. Thy-1 regulates fibroblast focal adhesions, cytoskeletal organization and migration through modulation of p190 RhoGAP and Rho GTPase activity. *Exp Cell Res* 2004; 295:488-496.
26. Dudas J, Mansuroglu T, Batusic D, Saile B, Ramadori G. Thy-1 is an in vivo and in vitro marker of liver myofibroblasts. *Cell Tissue Res* 2007; 329:503-514.
27. Ryder JW, Gordon JA. In vivo effect of sodium orthovanadate on pp60c-src kinase. *Mol Cell Biol* 1987; 7:1139-1147.
28. Welsh CF, Assoian RK. A growing role for Rho family GTPases as intermediaries in growth factor- and adhesion-dependent cell cycle progression. *Biochim Biophys Acta* 2000; 1471:M21-29.
29. Chang JH, Gill S, Settleman J, Parsons SJ. c-Src regulates the simultaneous rearrangement of actin cytoskeleton, p190RhoGAP, and p120RasGAP following epidermal growth factor stimulation. *J Cell Biol* 1995; 130:355-368.
30. Arthur WT, Petch LA, Burridge K. Integrin engagement suppresses RhoA activity via a c-Src-dependent mechanism. *Curr Biol* 2000; 10:719-722.
31. Kontaridis MI, Eminaga S, Fornaro M, Zito CI, Sordella R, Settleman J, et al. SHP-2 positively regulates myogenesis by coupling to the Rho GTPase signaling

- pathway. *Mol Cell Biol* 2004; 24:5340-5352.
32. Iwamoto H, Nakamuta M, Tada S, Sugimoto R, Enjoji M, Nawata H. A p160ROCK-specific inhibitor, Y-27632, attenuates rat hepatic stellate cell growth. *J Hepatol* 2000; 32:762-770.
 33. Murata T, Arii S, Mori A, Imamura M. Therapeutic significance of Y-27632, a Rho-kinase inhibitor, on the established liver fibrosis. *J Surg Res* 2003; 114:64-71.
 34. Choi SS, Sicklick JK, Ma Q, Yang L, Huang J, Qi Y, et al. Sustained activation of Rac1 in hepatic stellate cells promotes liver injury and fibrosis in mice. *Hepatology* 2006; 44:1267-1277.
 35. Machide M, Hashigasako A, Matsumoto K, Nakamura T. Contact inhibition of hepatocyte growth regulated by functional association of the c-Met/hepatocyte growth factor receptor and LAR protein-tyrosine phosphatase. *J Biol Chem* 2006; 281:8765-8772.
 36. Chao W, Liu H, Olson MS. Effect of orthovanadate on tyrosine phosphorylation of P120 GTPase-activating protein in rat liver macrophages (Kupffer cells). *Biochem Biophys Res Commun* 1993; 191:55-60.
 37. Moyer KE, Saba AA, Hauck RM, Ehrlich HP. Systemic vanadate ingestion modulates rat tendon repair. *Exp Mol Pathol* 2003; 75:80-88.
 38. Ehrlich HP, Keefer KA, Myers RL, Passaniti A. Vanadate and the absence of myofibroblasts in wound contraction. *Arch Surg* 1999; 134:494-501.
 39. Iredale JP. Models of liver fibrosis: exploring the dynamic nature of

- inflammation and repair in a solid organ. *J Clin Invest* 2007; 117:539-548.
40. French RJ, Jones PJ. Role of vanadium in nutrition: metabolism, essentiality and dietary considerations. *Life Sci* 1993; 52:339-346.
41. al-Bayati MA, Giri SN, Raabe OG, Rosenblatt LS, Shifrine M. Time and dose-response study of the effects of vanadate on rats: morphological and biochemical changes in organs. *J Environ Pathol Toxicol Oncol* 1989; 9:435-455.
42. Wenzel UO, Fouqueray B, Biswas P, Grandaliano G, Choudhury GG, Abboud HE. Activation of mesangial cells by the phosphatase inhibitor vanadate. Potential implications for diabetic nephropathy. *J Clin Invest* 1995; 95:1244-1252.
43. Heffetz D, Bushkin I, Dror R, Zick Y. The insulinomimetic agents H₂O₂ and vanadate stimulate protein tyrosine phosphorylation in intact cells. *J Biol Chem* 1990; 265:2896-2902.
44. Jaeschke H. Mechanisms of Liver Injury. II. Mechanisms of neutrophil-induced liver cell injury during hepatic ischemia-reperfusion and other acute inflammatory conditions. *Am J Physiol Gastrointest Liver Physiol* 2006; 290:G1083-1088.

Figure legends

Fig. 1. Dose-dependent inhibition of cultured rat HSCs by OV. Cultured for 7 days. **A:** Phase-contrast micrographs (with a 10x objective). **B:** DNA fluorometric quantification of cell number in HSC culture. Each data point is expressed as percentage of control (means \pm SEM for five independent experiments). *, $p < 0.05$; ***, $p < 0.001$; compared with control; one-way ANOVA (analysis of variance).

Fig. 2. Maintenance of the stellate shape with few stress fibers and the capacity for retinoid uptake in OV-treated HSCs. Cultured for 14 days. From the top, phase-contrast microscopy, rhodamine-phalloidin staining for F-actin, ultraviolet (UV) autofluorescence of retinoid (cultured in the presence of 10 μ M retinol), and α -Smooth muscle actin immunocytochemistry. With a 20x objective.

Fig. 3. Suppressed expression of α -SMA, PCNA, and type I collagen mRNA in cultured HSCs in the presence of OV. **A:** Western blot analysis of expression of α -SMA, desmin, vimentin, PCNA, and GAPDH in freshly isolated HSCs (0 day) and cultured HSCs (cultured for 3 days or 7 days). **B:** RT-PCR analysis of gene expression of collagen type I α (Coll-I α), fibronectin, plasminogen activator inhibitor-I (PAI-I), peroxisome proliferator-activated receptor γ (PPAR γ), and c-Myb.

Fig. 4. Partial recovery of quiescent phenotype in activated HSCs after OV treatment. HSCs were cultured for 7 days, after which OV (20 μ M) was applied (total culturing period: 14 days). **A:** Phase-contrast micrographs (with a 10x objective). **B:** Analysis of expression of α -SMA, desmin, vimentin, and PCNA (Western blotting) and type I collagen mRNA (RT-PCR).

Fig. 5. Effect of OV on protein tyrosine phosphorylation and several signaling molecules regulated by phosphorylation in cultured HSCs. **A:** Western blot analysis of tyrosine phosphorylated proteins in HSCs cultured in the absence or presence of OV (20 μ M). **B:** Western blot analysis of phosphorylation status of ERK, p190RSK, Akt, Stat3, p38 MAPK, and CREB.

Fig. 6. Induction of Src phosphorylation at Tyr-527 by OV and partial abrogation of OV's effect by a Src-specific inhibitor in cultured HSCs. **A:** Western blot analysis of total Src and tyrosine phosphorylated Src (Tyr-416 and Tyr-527). HSCs were cultured for 7 days (lanes 2 and 3) or 14 days (lanes 4 and 5). OV (20 μ M) was applied at the start of culture (lane 3) or after 7 days (lane 5). **B:** Phase-contrast micrographs (with a 10x objective). HSCs were cultured for 7 days with or without OV in the presence of the Src inhibitor PP2 (10 μ M) or vehicle control (dimethylsulfoxide). **C:** Western blot analysis of α -SMA, phosphorylated Src (Tyr-416), and total Src. HSCs were first cultured for 10 days, after which OV and PP2 were added and further cultured for 7 days.

Fig. 7. Activation of the Rho family proteins in cultured HSCs and its inhibition by OV.

A: Western blot analysis of Rho, Rac, and Cdc42. HSCs were cultured for a total period of 18 days. OV (20 μ M) was added after 11 days. **B:** Phase-contrast micrographs of HSCs treated with OV or Y-27632 (with a 10x objective).

Fig. 8. Suppression of HSC activation by systemic administration of OV in an acute CCl₄

injury model. Single administration of CCl₄. **A:** Hematoxylin and eosin staining and α -SMA and desmin immunohistochemistry of the liver (with a 10x objective) after 72 hours. **B:** Quantitative analysis of α -SMA-immunoreactivity (left panel) and desmin-immunoreactivity (right panel). Each data point represents mean \pm SEM for nine (control) and six (CCl₄ and CCl₄ + OV) rats. ***, $p < 0.001$ as compared with CCl₄ alone at 72 hours; one-way ANOVA (analysis of variance).

Fig. 9. Amelioration of liver injury and suppression of fibrosis by systemic

administration of OV in a chronic CCl₄ injury model. Repeated administration of CCl₄ for 8 weeks. OV was intraperitoneally injected three times per week at the indicated doses. **A:** Gross appearances of the livers (scale bar, 1 cm). **B:** Serum levels of ALT and ALP. The number in parentheses indicates the dose of OV (mg/kg). Each data point represents mean \pm SEM for eight rats. ***, $p < 0.001$; compared with CCl₄ alone; ANOVA. **C:** Sirius red staining of the liver (with a 10x objective). **D:** Quantitative analysis of

sirius red-positive area. The number in parentheses indicates the dose of OV (mg/kg). Each data point represents mean \pm SEM for eight rats. **, $p < 0.01$; ***, $p < 0.001$; compared with CCl₄ alone; one-way ANOVA (analysis of variance).

Fig. 10. Amelioration of liver injury and suppression of HSC activation in a chronic DMN injury model (5 weeks). **A:** Gross appearances of the livers (scale bar, 1 cm). **B:** Serum levels of ALT and ALP (mean \pm SEM) for six rats. The number in parentheses indicates the dose of OV (mg/kg). ***, $p < 0.001$; compared with DMN alone; ANOVA. **C:** Sirius red staining and α -SMA immunohistochemistry of the liver (with a 10x objective). **D:** Quantitative analysis of α -SMA-immunoreactivity within the liver lobules (mean \pm SEM) for six rats. The number in parentheses indicates the dose of OV (mg/kg). **, $p < 0.01$; ***, $p < 0.001$; compared with DMN alone; one-way ANOVA (analysis of variance).

Supplemental Fig. 1. Time course of the increases in the levels of serum ALT after acute CCl₄ injury. Serum levels of ALT were measured prior to the injury and 24, 48, and 72 hrs after the injury. A 1:1 mixture of CCl₄ and olive oil (or olive oil for control) was administered by gavage at a dose of 3 ml/kg body weight. OV (5 mg/kg) or saline was injected intraperitoneally at 30 minutes before the injury. For animals sacrificed after 48 and 72 hrs, OV (5 mg/kg) or saline was also injected after 24 hrs. For animals

sacrificed after 72 hrs, an additional injection of OV or saline was performed after 48 hrs.

Each data point represents mean \pm SEM for four rats.

Supplemental Fig. 2. Histology of the major organs in control and chronically OV-treated animals. **A-P:** Hematoxylin and eosin staining. **A-D:** liver; **E-H:** pancreas; **I-L:** kidney; **M-P:** spleen. **A, C, E, G, I, K, M, O:** with a 10x objective; **B, D, F, H, J, L, N, P:** with a 40x objective. **A, B, E, F, I, J, M, N:** control (saline); **C, D, G, H, K, L, O, P:** OV (5 mg/kg, intraperitoneally, three times per week for 8 weeks).

Figure 1 (Nishikawa et al.)

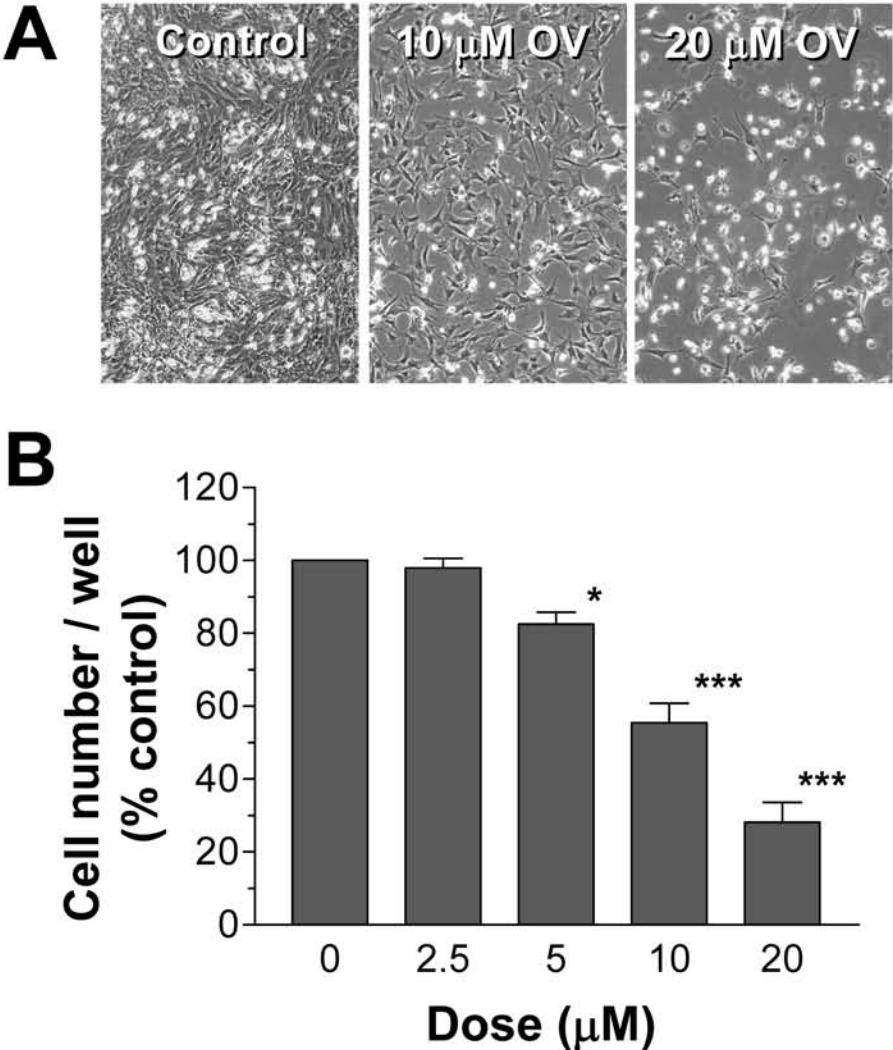


Figure 2 (Nishikawa et al.)

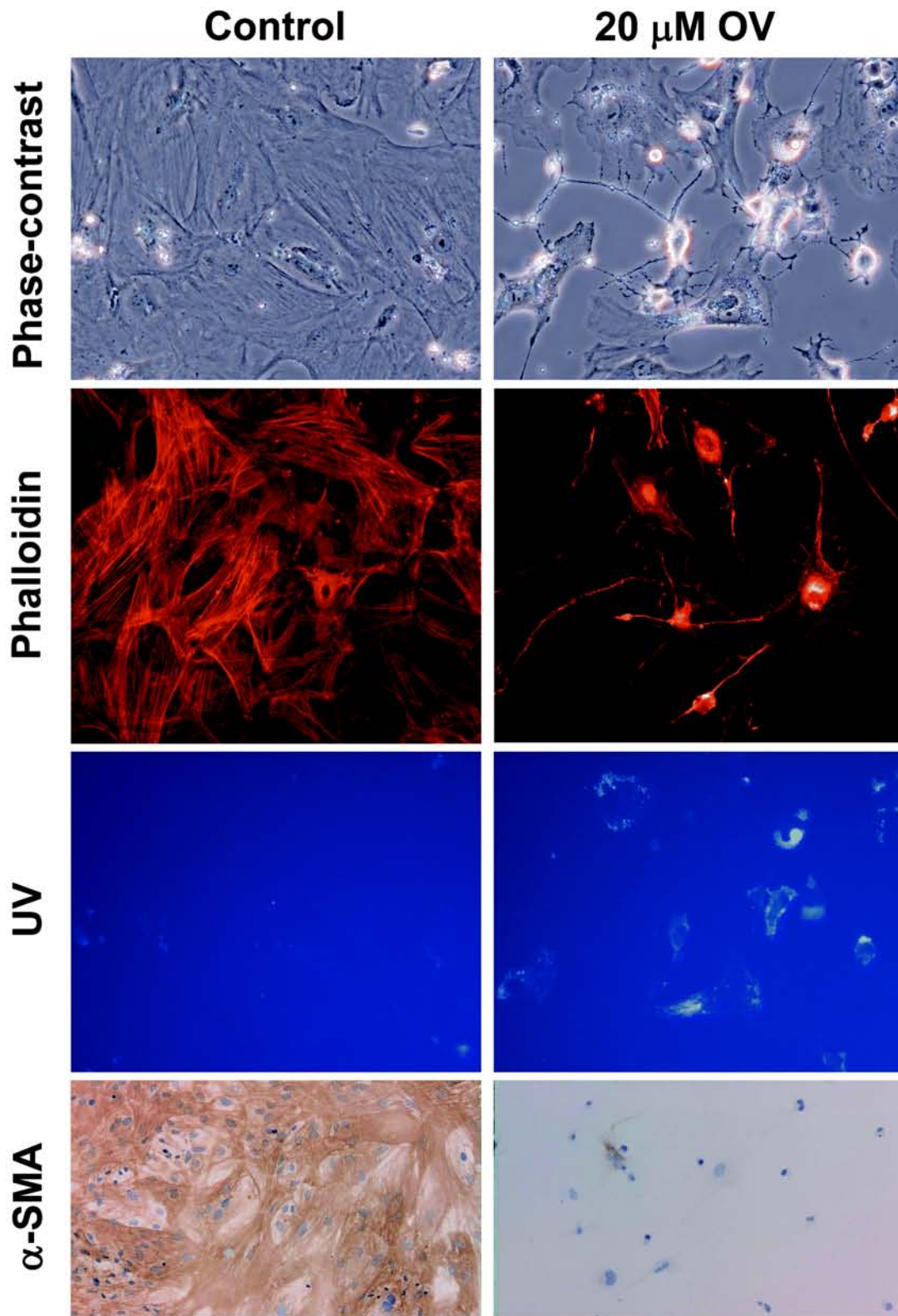


Figure 3 (Nishikawa et al.)

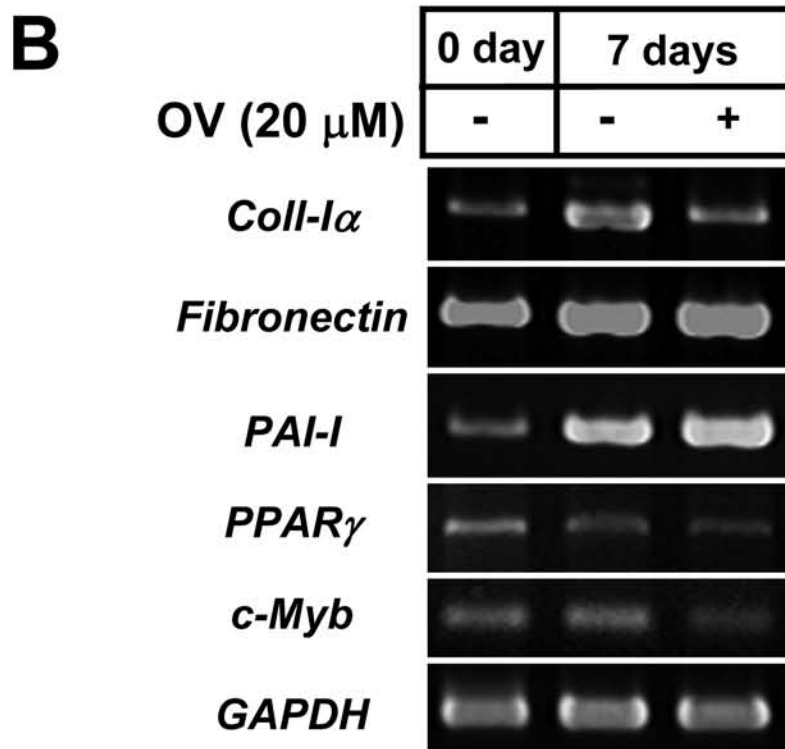
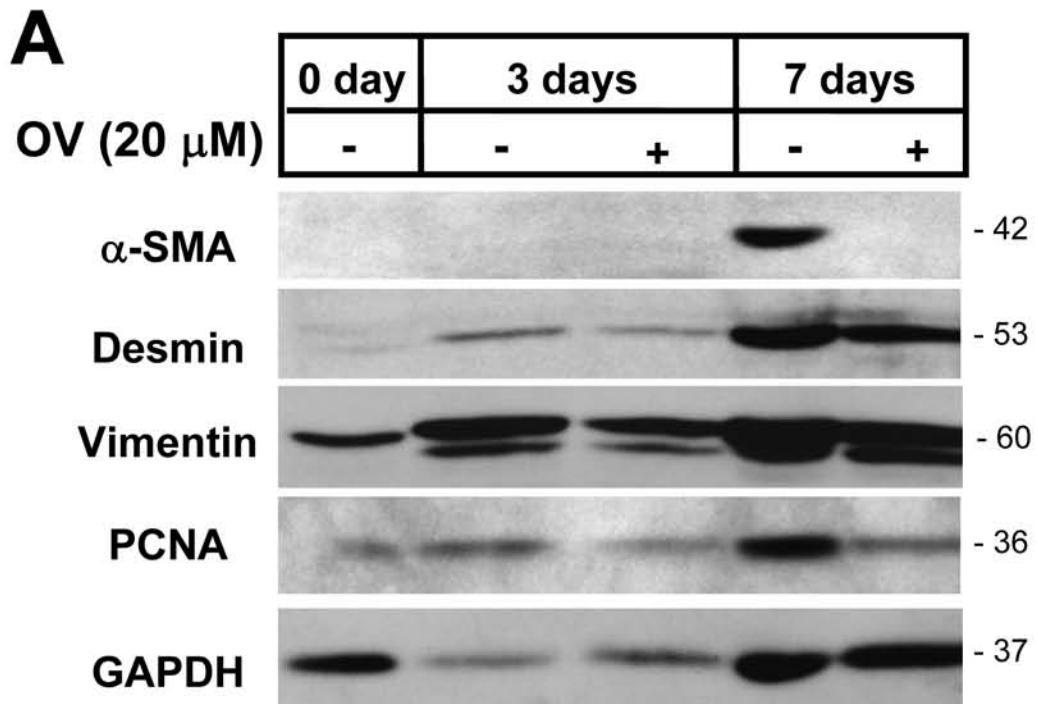


Figure 4 (Nishikawa et al.)

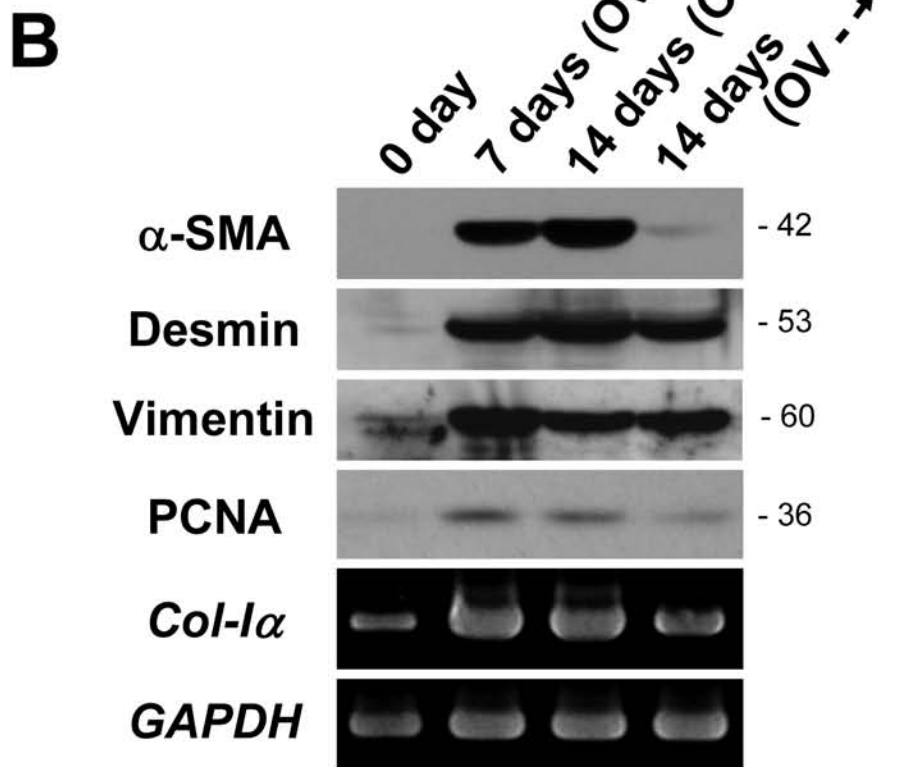
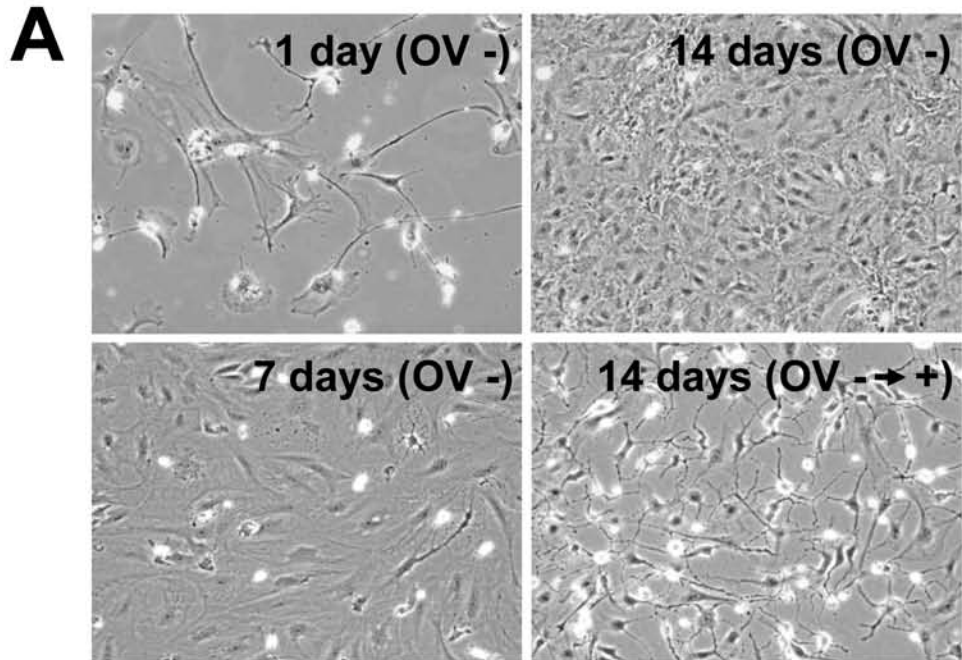


Figure 5 (Nishikawa et al.)

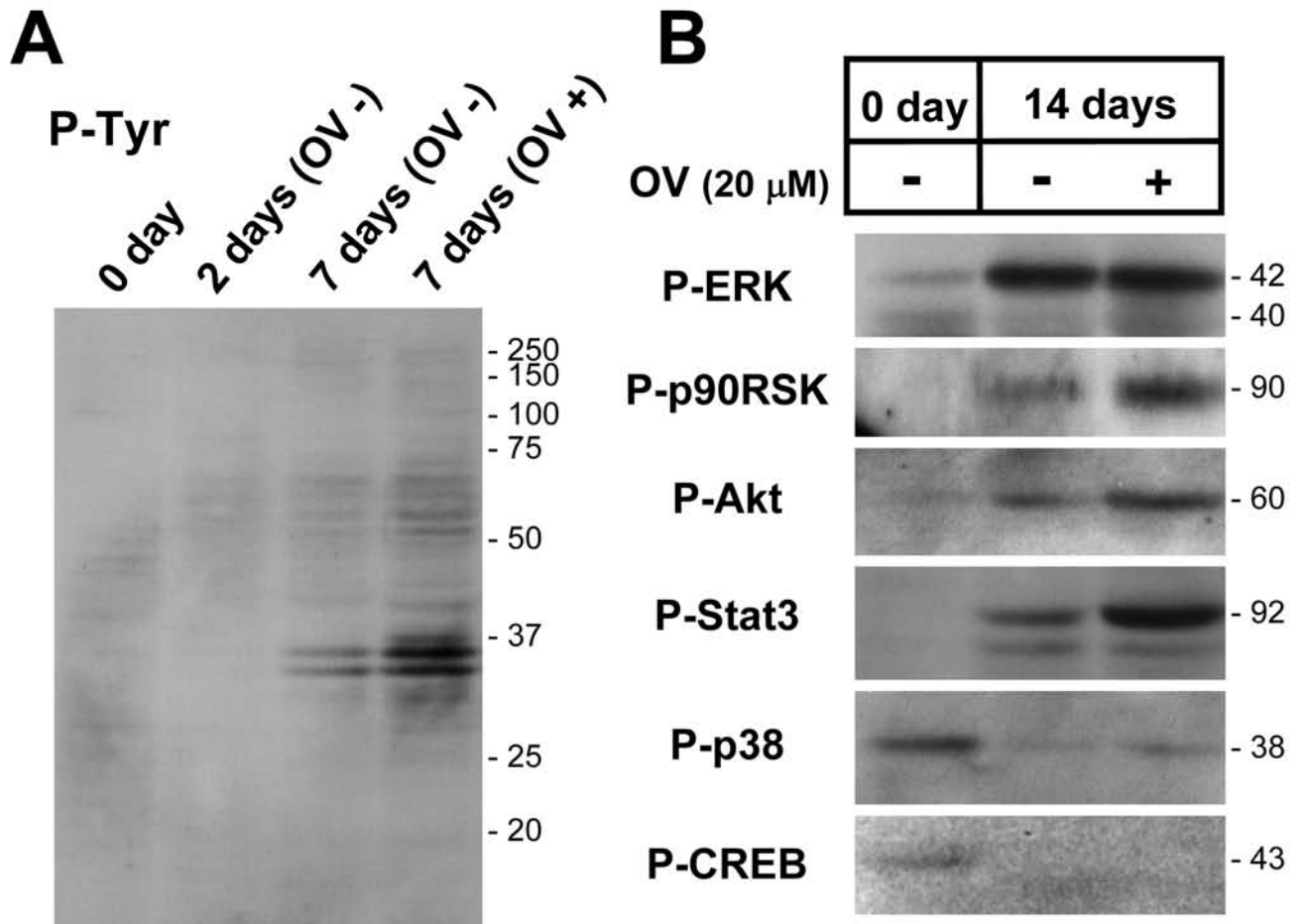


Figure 6 (Nishikawa et al.)

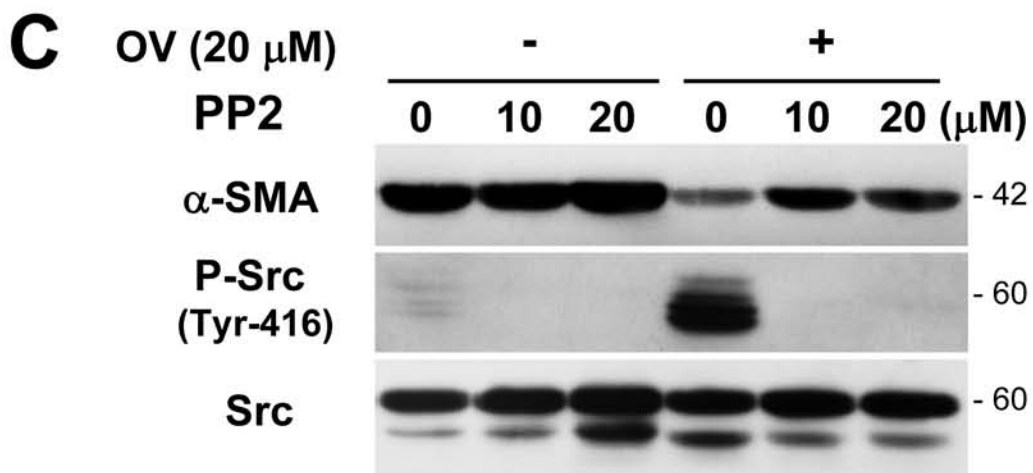
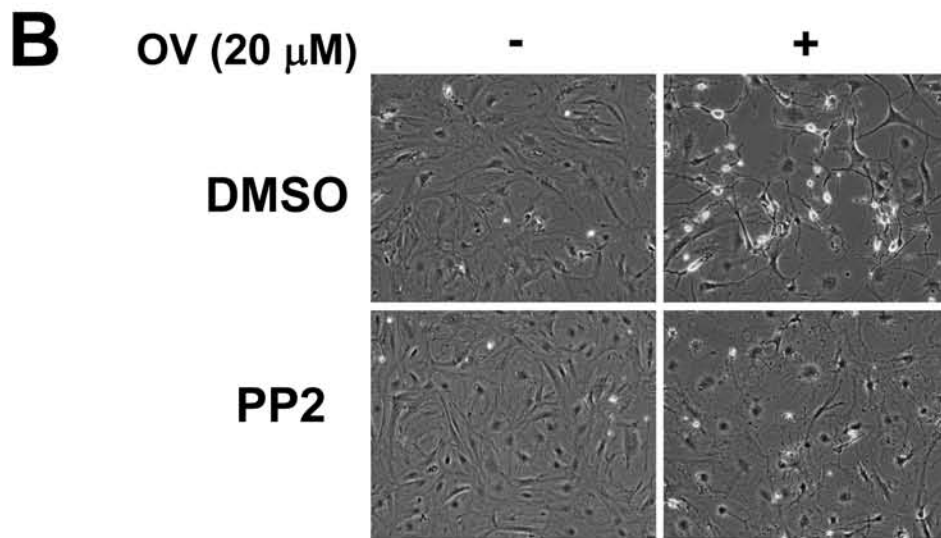
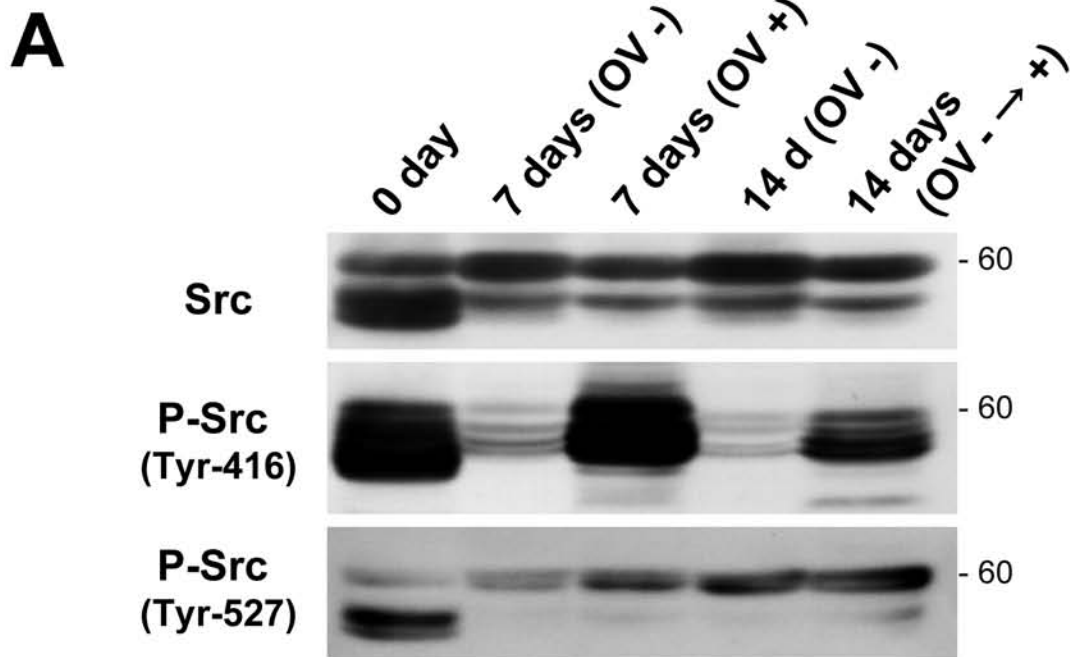


Figure 7 (Nishikawa et al.)

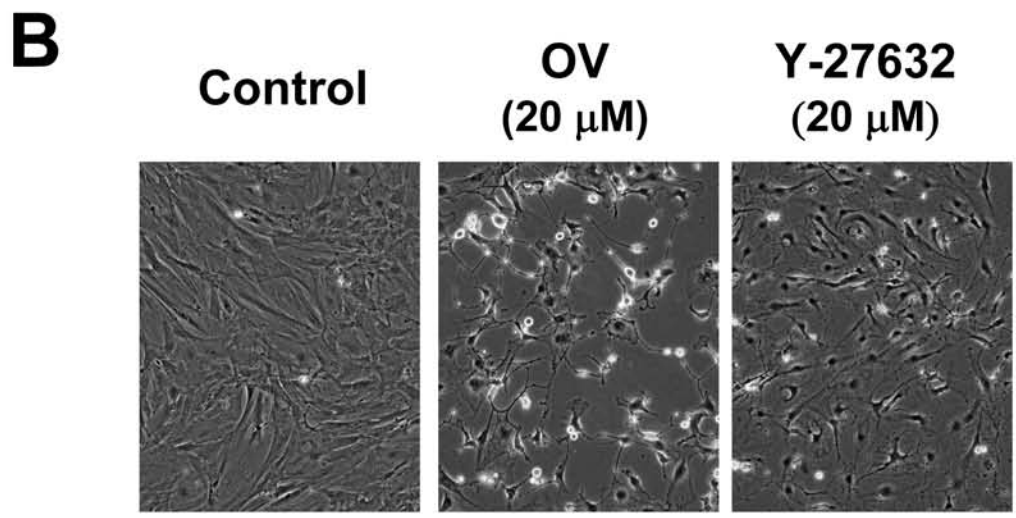
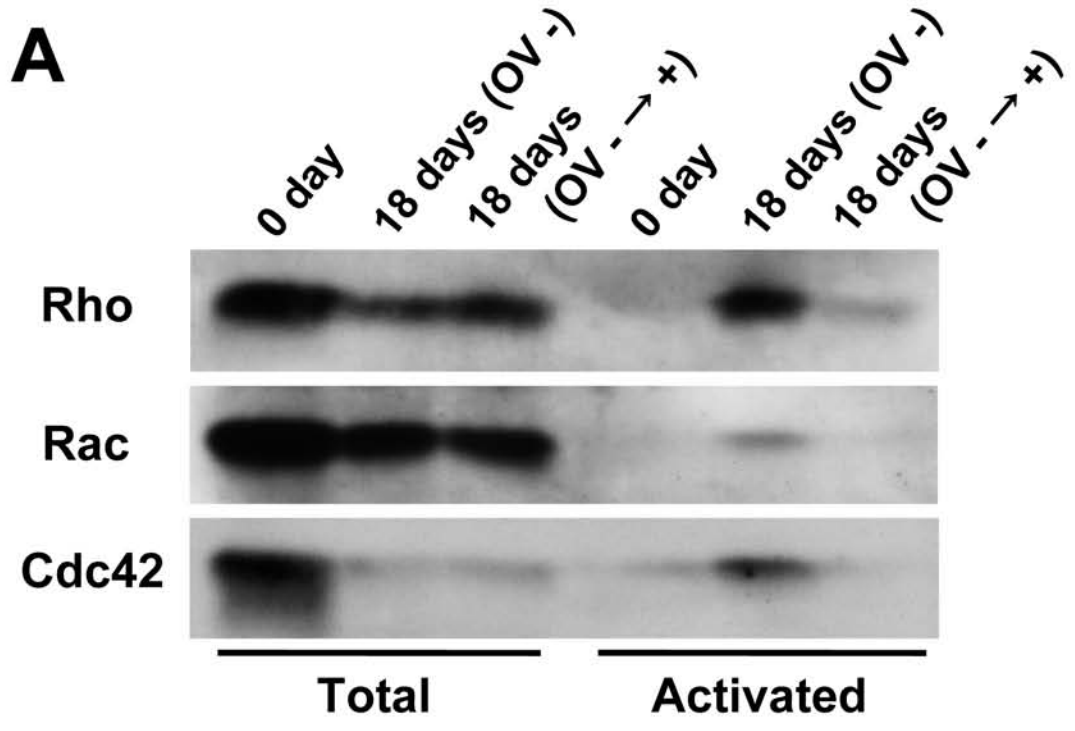


Figure 8 (Nishikawa et al.)

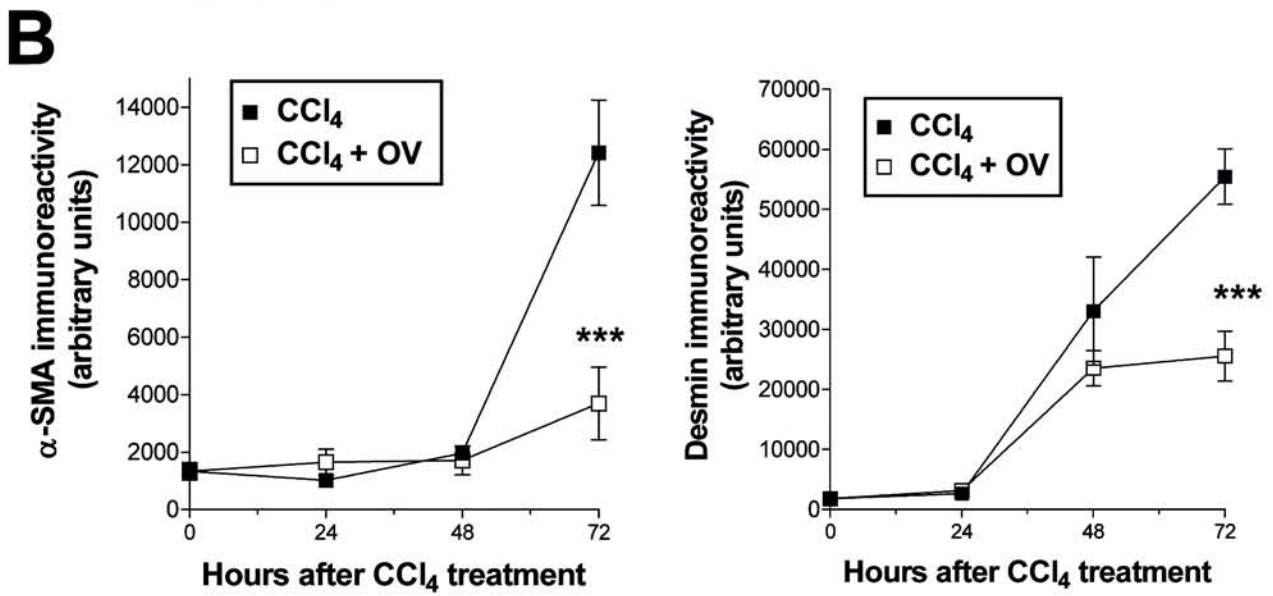
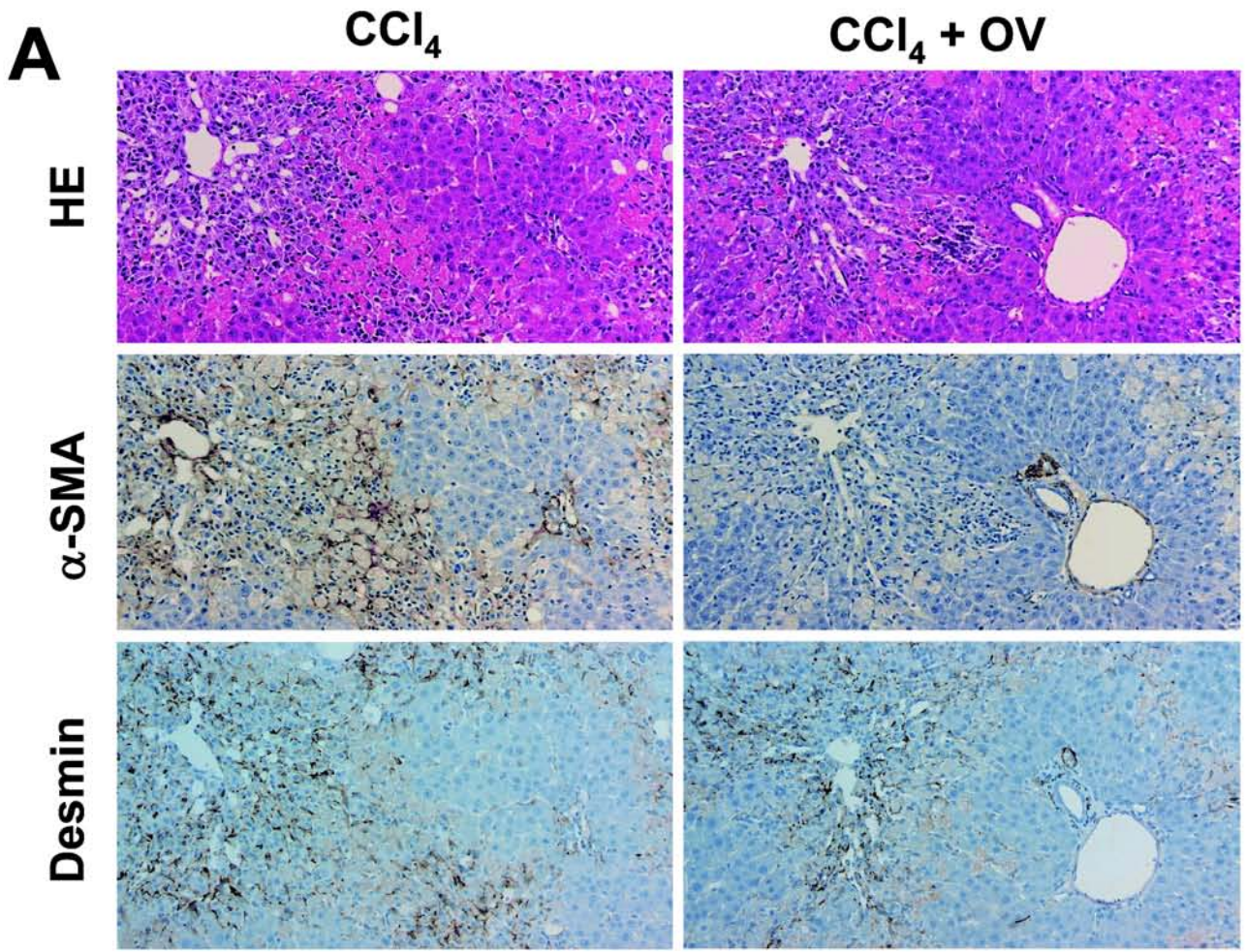


Figure 9 (Nishikawa et al.)

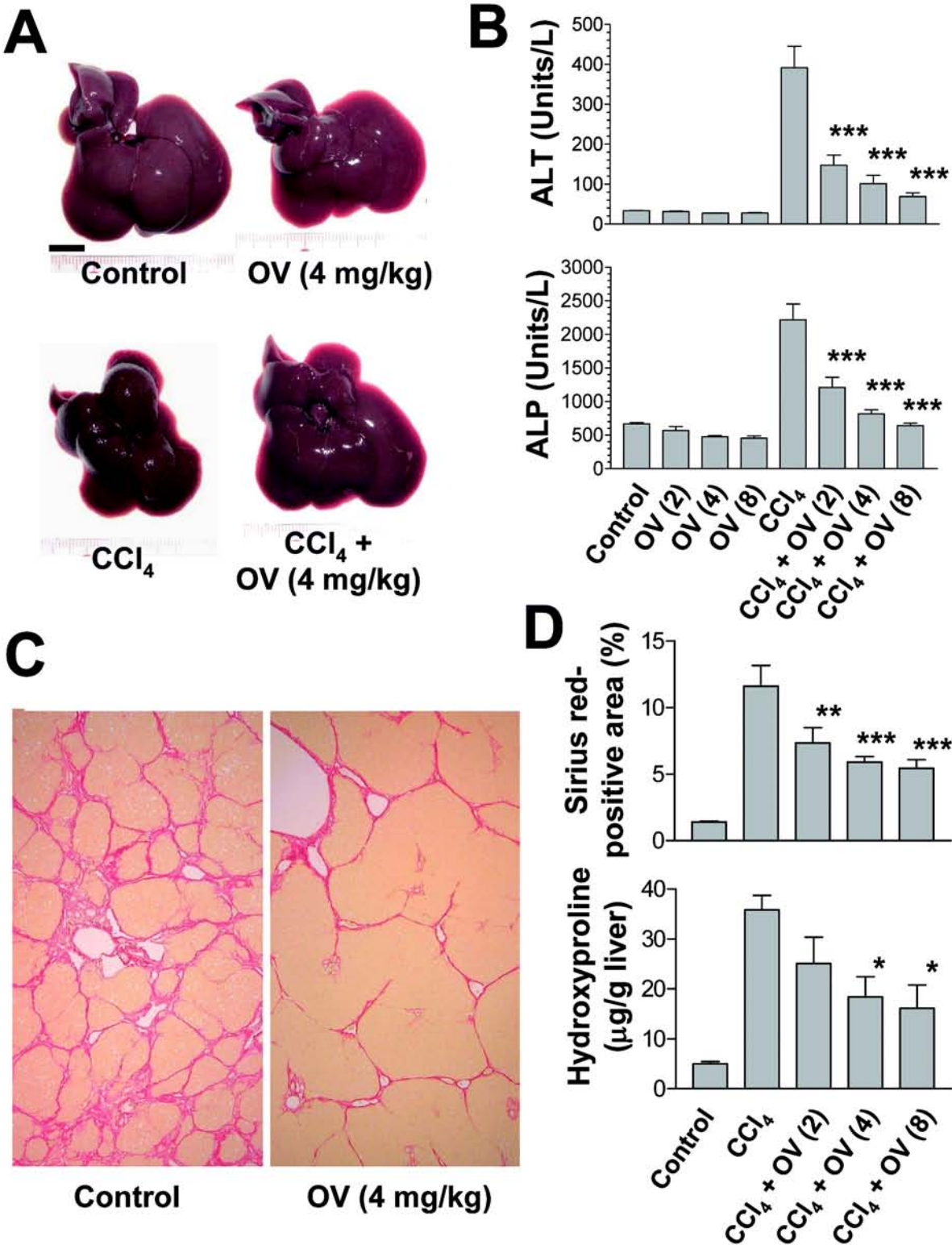


Figure 10 (Nishikawa et al.)

